

University of New Mexico
UNM Digital Repository

Earth and Planetary Sciences ETDs

Electronic Theses and Dissertations

12-1-2010

New structural interpretation, microstructural analyses, and preliminary monazite geochronology of Proterozoic rocks in the central Manzano Mountains, New Mexico

Steve A. Rogers

Follow this and additional works at: https://digitalrepository.unm.edu/eps_etds

Recommended Citation

Rogers, Steve A.. "New structural interpretation, microstructural analyses, and preliminary monazite geochronology of Proterozoic rocks in the central Manzano Mountains, New Mexico." (2010). https://digitalrepository.unm.edu/eps_etds/73

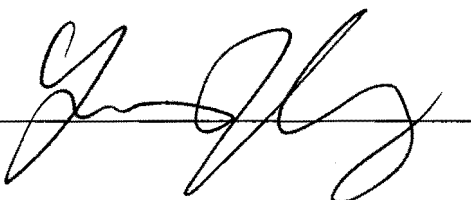
This Thesis is brought to you for free and open access by the Electronic Theses and Dissertations at UNM Digital Repository. It has been accepted for inclusion in Earth and Planetary Sciences ETDs by an authorized administrator of UNM Digital Repository. For more information, please contact disc@unm.edu.

**New Structural Interpretation, Microstructural Analyses, and Preliminary
Monazite Geochronology of Proterozoic Rocks in the Central Manzano Mountains,
New Mexico**

Honors Thesis

Rogers, Steven A., captainamerica520@hotmail.com

Dr. Karl Karlstrom 

Dr. Laura Crossey 

Dept. of Earth and Planetary Sci., UNM, Albuquerque, NM 87131

Abstract

The Manzano Mountains of central New Mexico, on the east flank of the Rio Grande rift, provide excellent outcrops of Proterozoic basement. Rock types in the area include Sevilleta metarhyolite, amphibolitic metavolcanic rocks, schist, meta-lithic arenite, banded metarhyolite, the White Ridge and related quartzites, and the Blue Springs schist. Plutonic activity included the emplacement of the Monte Largo (1656Ma) and Priest (1427Ma) plutons. Proterozoic metavolcanic and metasedimentary rocks were multiply deformed during at least three deformation events. D1, D2, D3 of rocks in the Manzano Mountains have all produced movement along the NE striking Monte Largo shear zone (MLSZ). The movement sense within this shear zone is consistently top-to-the-northwest. Analysis of microstructures from the MLSZ, combined with studies of overprinting relationships of folded rocks of the area provides a better understanding of the kinematics associated with each deformation event. Geochronologic studies of metamorphic monazite grains will place time constraints on when movement occurred within the area. Metamorphic monazite grown during tectonic deformation can have incremental growth patterns such as rim and core features. The ability to relate grain orientation to overall fabric of the rocks combined with the ability to obtain geochronological information of individual grains (and individual parts of each grain, i.e rim/core features) helps in interpreting how and when deformation occurred.

Examination of thin sections of quartzites within the MLSZ as well as from the folded quartzites within the metasedimentary package provides information to help understand the kinematics and time constraints of each deformational event.

Introduction

Evaluation of Proterozoic structures and tectonic evolution in the southwestern US can help to elucidate the process of continental assembly that went on to build North America and the processes of subsequent reactivation of existing structures in North America. Proterozoic exposures in the SW form a 1300km wide orogenic belt that was built by assembly of oceanic terranes between 1.8 and 1.6 GA (Karlstrom and Bowring, 1988). In particular the Proterozoic rocks within central New Mexico have been defined to lie within the Mazatzal province, which was assembled during the Mazatzal orogenic event c.a.1.65-1.60 Ga (Bowring and Karlstrom, 1990).

This study evaluates part of the Manzano thrust belt system which documents episodes of thrust sense deformation. In particular, the Monte Largo shear zone is a regionally important structure that has had progressive Proterozoic movement with important deformation occurring at ~1.65 and 1.42GA. Using techniques such as detailed geologic mapping, microstructural analyses, and preliminary in situ Monazite dating, this paper presents an assessment of structural characteristics and timing of deformation in this region. Work was done as part of the New Mexico State map effort on the Capilla Peak Quadrangle. Approximately two full months were spent in mapping and structural studies and mapping results were presented in part in the Geologic Quadrangle of the Capilla Peak (Karlstrom et al. 2001).

Previous Work

The Manzano Mountains are a N-S trending, mountain uplift that contains excellent exposure of Proterozoic outcrops, unconformably overlain by flat lying to shallowly east dipping Paleozoic rocks. The Manzano thrust system is a series of N-NE trending, SE dipping Precambrian thrusts within the ~70km long mountain range (Figure 1). Mapped within the Capilla Peak Quadrangle, the Monte Largo Shear Zone was first named and briefly described by Bauer (1982) as a 2m wide ductile fault. Subsequent work has been completed by Thompson et al. (1996) and Raszewski (1999) who recognized it as a wider zone of shear (on the order of 2km) and furthermore recognized top-to-the-northwest movement sense.

Proterozoic rock types within the Capilla Peak Quadrangle include both felsic and mafic metavolcanic, metalithic arenite, and complexly interbedded clean quartzites, schists, and a banded metarhyolite. Due to the complex deformation history, a coherent stratigraphic sequence has been difficult to ascertain. However, regional mapping suggest the following sequence: Metarhyolite (Xr), amphibolites (Xa), pelitic schist (Xps), meta-lithic arenite (Xla), quartzites (Xq), a banded metarhyolite (Xbr), and the Blue Springs schist (Xbs), as well as two intrusive granites of the Ojito, Monte Largo, and Priest plutons, the latter being south of the Capilla Peak Quadrangle (Karstrom, et al., 2001) (see Appendix B for illustrated stratigraphic sequence).

Metamorphism within the Proterozoic rocks in the field area was different grades above and below the MLSZ. The footwall of the MLSZ thrust is of greenschist grade, whereas the hanging wall is of amphibolite grade metamorphism. The MLSZ has juxtaposed regionally metamorphosed rocks by thrusting higher-grade rocks on top of

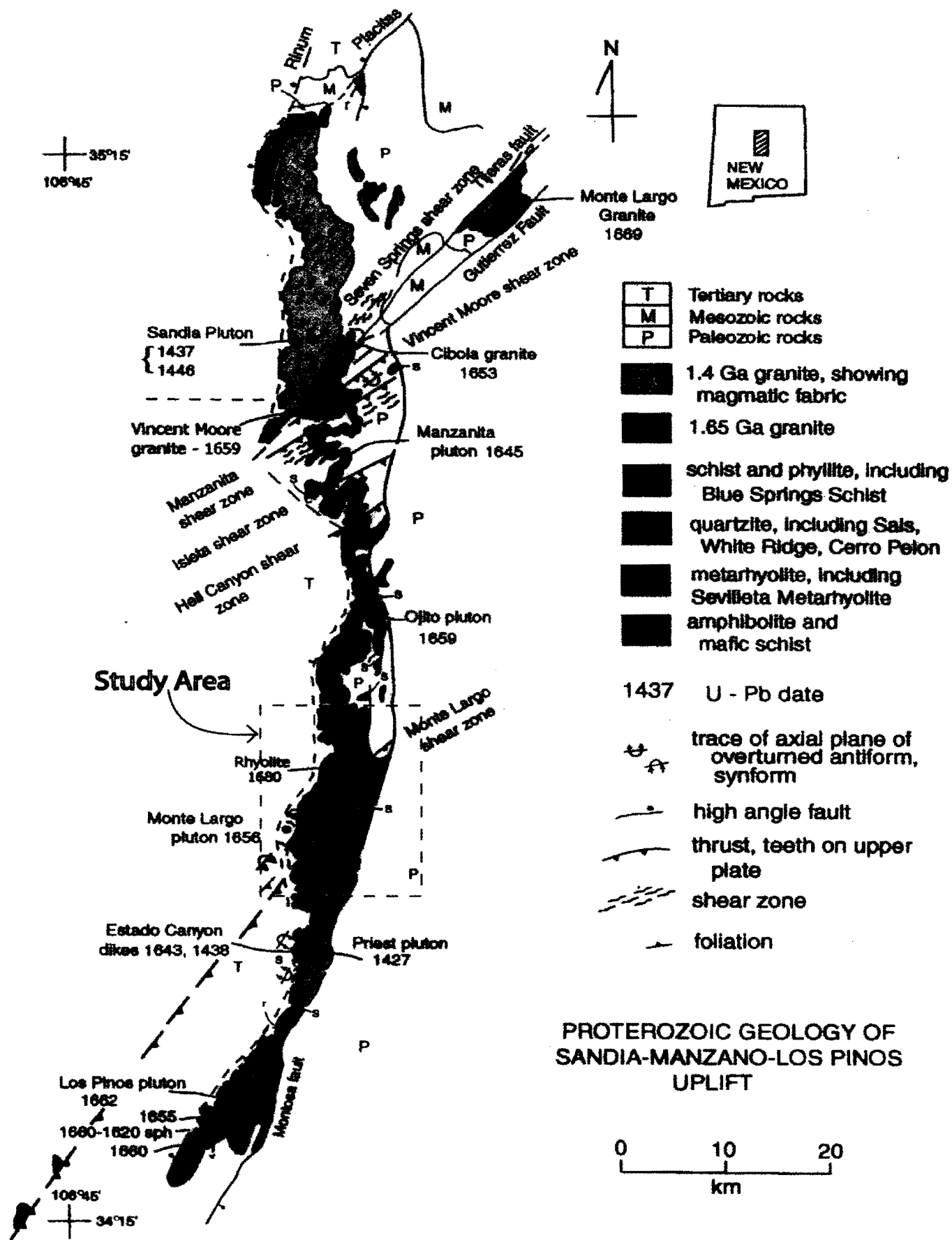


Figure 1: Regional map of Manzano mountains, showing generalized rock type distributions, with some geochronology, and major structures; including Manzano Thrust belt (NE trending Pc thrusts/shear zones) and the MLSZ, located within highlighted study area of the Capilla Peak Quad. (Figure courtesy of K. Karlstrom)

lower grade rock. Thompson (1991) reported based on garnet-biotite geothermometry that the footwall of the MLSZ is of greenschist facies metamorphism (~485°C) and that the hanging wall of the shear zone is of lower amphibolite facies (~530°C).

Regional plutonic activity within the Capilla Peak Quadrangle is displayed by the presence of two bodies of intrusive granitoids. The Monte Largo granodiorite has a U-Pb zircon date of 1656±10Ma (Bauer et al., 1993) and the Ojito, a quartz monzonite has a U-Pb zircon date of 1659±5Ma (Unruh, unpublished data). The emplacement of these granitic plutons are synchronous with North American continental assembly during the Mazatzal orogeny, ~1690-1630Ma (Karlstrom and Bowring, 1988). There has been significant younger plutonic activity within the region as well. The Sandia and Priest pluton granitoids have emplacement ages of ~1.44 and 1.42 Ga, respectively. (Bauer, et al., 1993; Bauer and Pollock, 1993). The Sandia granite is present ~35km north of the study area and the Priest pluton is exposed a few km south.

Accompanying the polyphase deformational history of these rocks is a noted history of a significant occurrence of fluid interaction within the study area. Northrup, 1991, reported the occurrence of at least 7 types of veins within the rocks surrounding the MLSZ. The presence of this suite of veins of various silicious compositions emphasizes the fact that there has been major fluid activity during Proterozoic tectonic activity.

Structural Interpretation

This section describes new structural mapping within the Capilla Peak Quadrangle. Folds, faults and shear zones in the Capilla Peak Quadrangle exhibit several styles of deformation related to different periods of tectonic activity. Figure 2 is a

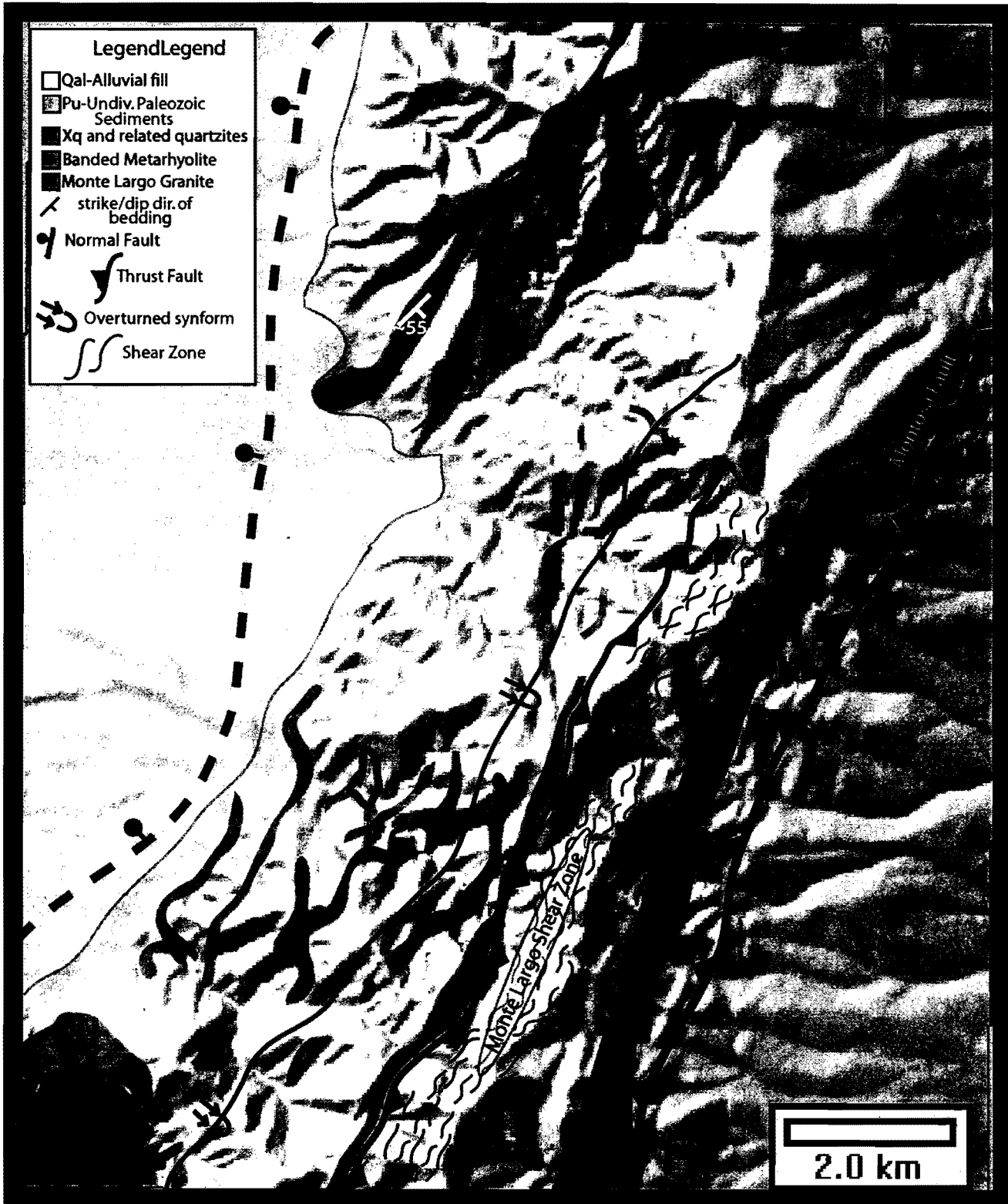


Figure 2: Schematic map of the Capilla Peak Quadrangle, NM. Major rock type distributions as well as major structural features are represented.

schematic map of the Capilla Peak geology, which portrays the distribution of the major rock types, and the major structural features of the area (for a more detailed map, see inserted Appendixed Geological Quadrangle map)

Paleozoic and Younger Structures

Phanerozoic structures consist primarily of faults and gentle- to steep- limbed drape or monoclinial folds adjacent to these faults. Most faults strike N-S with minor bends and splays that strike NNE and NNW. Several faults within the Capilla Peak Quadrangle likely had complex movement histories associated with contraction of the Laramide orogeny in late Cretaceous/early Tertiary time and extension related to the development of the Rio Grande rift in late Oligocene/early Miocene.

The main fault system on the east side of the Manzano Mountains is the Montosa fault and related structures. These are interpreted to be of Laramide age based on their contractional character as west-side-up reverse faults. These faults have associated east-facing monoclines in the Paleozoic strata as shown in the NW-SE cross section (in Appendix). Total vertical separation on these structures is several thousand feet. The Montosa fault system dips west ~60-70°.

The west side of the Manzano Mountains is controlled by major, down-to-the-west, range-bounding faults that record dip-slip normal displacement associated with extension along the Rio Grande rift in Miocene time. Similar to the Hubbell bench to the north, the immediate range bounding faults in this part of the rift have only moderate vertical separation (7000-9000') and Mesozoic rocks are preserved near the range front. Younger sediments of the Santa Fe Group in general, conceal the traces of these faults.

Additionally, no clear evidence of Quaternary faulting was found in the Capilla Peak Quadrangle.

Proterozoic Structures

The character of Proterozoic structures is illustrated in the cross sections (in Appendix). Metamorphic and plutonic rocks are ductily deformed and show evidence for multiple generations of deformation. At least three deformation generations are recognized: D1, D2, and D3. The main tectonic fabric is a penetrative foliation (S2) that strikes N-NE (Figure 3b) throughout the quadrangle, parallel to the regional trend. S2 foliations are generally steeply dipping with both NW and SE dips. S1 is interpreted to be a transposition layering, now sub-parallel with original bedding, S0, associated with sub-horizontal thrusting during D1. F1 fold closures are rare where found, are asymmetric and they are NW verging and are tight to isoclinal and are subsequently refolded by F2 folds (Figure 4 & 5). F2 folds in the Capilla Peak area are N-NE trending (Figure 3a), plunging generally to the NE and are broad to tight upright asymmetric folds (and also verge to NW). Due to general attitude and overprinting relationships, most folds within the quadrangle are interpreted to be F2, although some may be F1 folds rotated into F2 orientations. F3 folds are a group of structures that fold, kink, or deflect the main S2 schistosity. In the southern part of the quadrangle, these include brittle-ductile thrusts with top-to-the northwest shear sense (Bauer et al., 1993). There is also an example of brittle-ductile thrust in the northern part of the quadrangle at the contact between lithic arenite schist and quartzite (Johnson, 1986) is interpreted to represent semi-brittle thrust displacements related to movement along the Monte Largo shear zone.

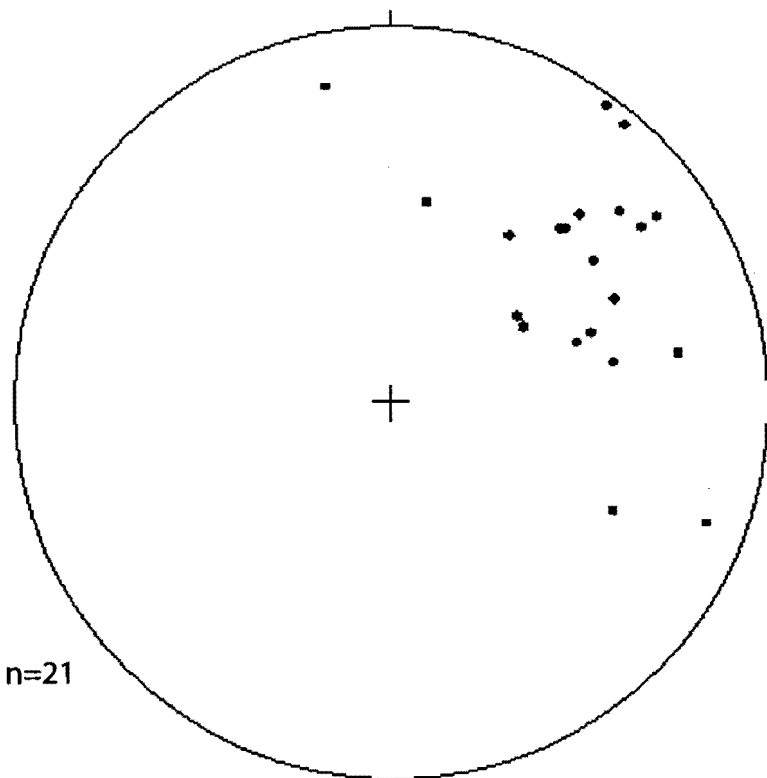
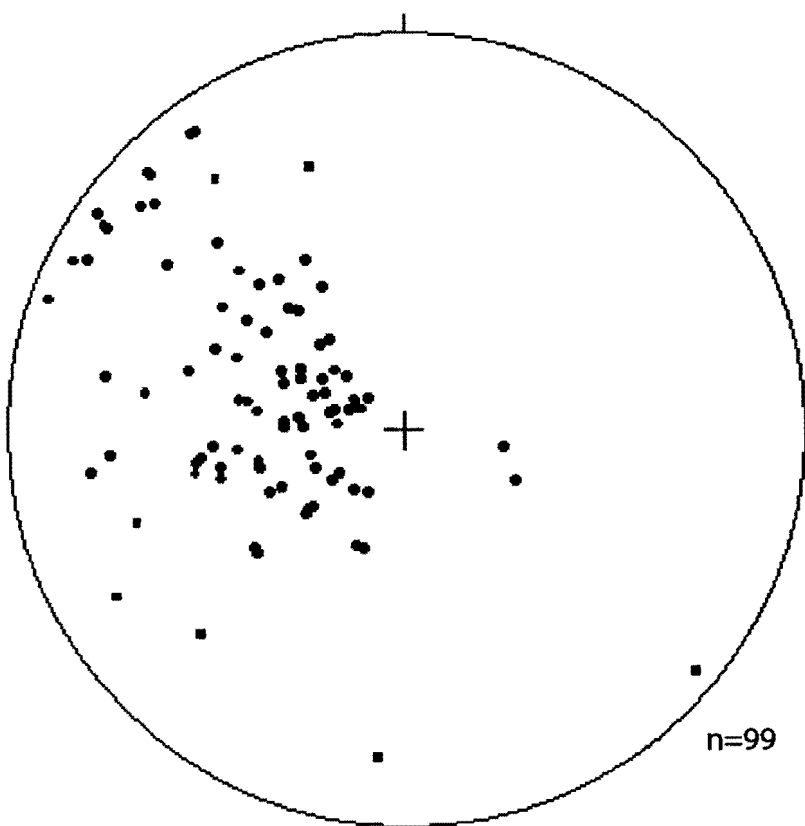


Figure 3a: Data plot of F2 axes. F2 folds trend to the NE, generally, and verge to the NW, based on examination of fold geometries. This NE trend of f2 folds is consistent with regional trends of similar generation deformation.

Figure 3b: Data plot of S2 foliation planes. Plot is poles to foliation. Foliation is N-NE striking, generally steep to shallow and has both NW and SE dips. S2 is subsequently deflected by rare F3 folds. Based on general attitudes, most folds within the Capilla Peak Quad. are interpreted to be F2.



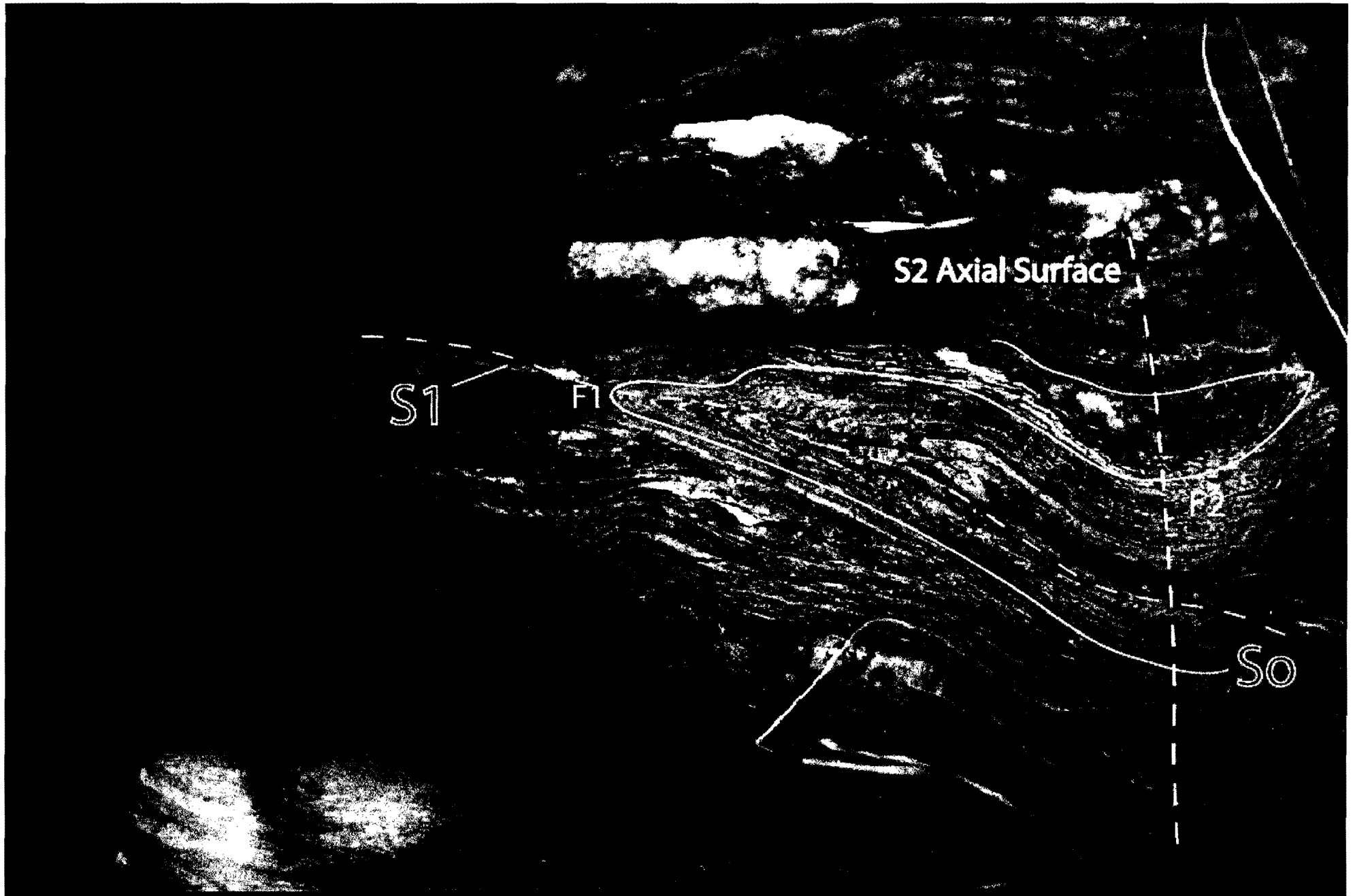


Figure 4: Photo of folded S1 fabric refolded by F2. The direction of the photo is looking to the NE, parallel to main fabric, S2. Rock type is Banded metarhyolite. (Photo courtesy of K. Karlstrom)

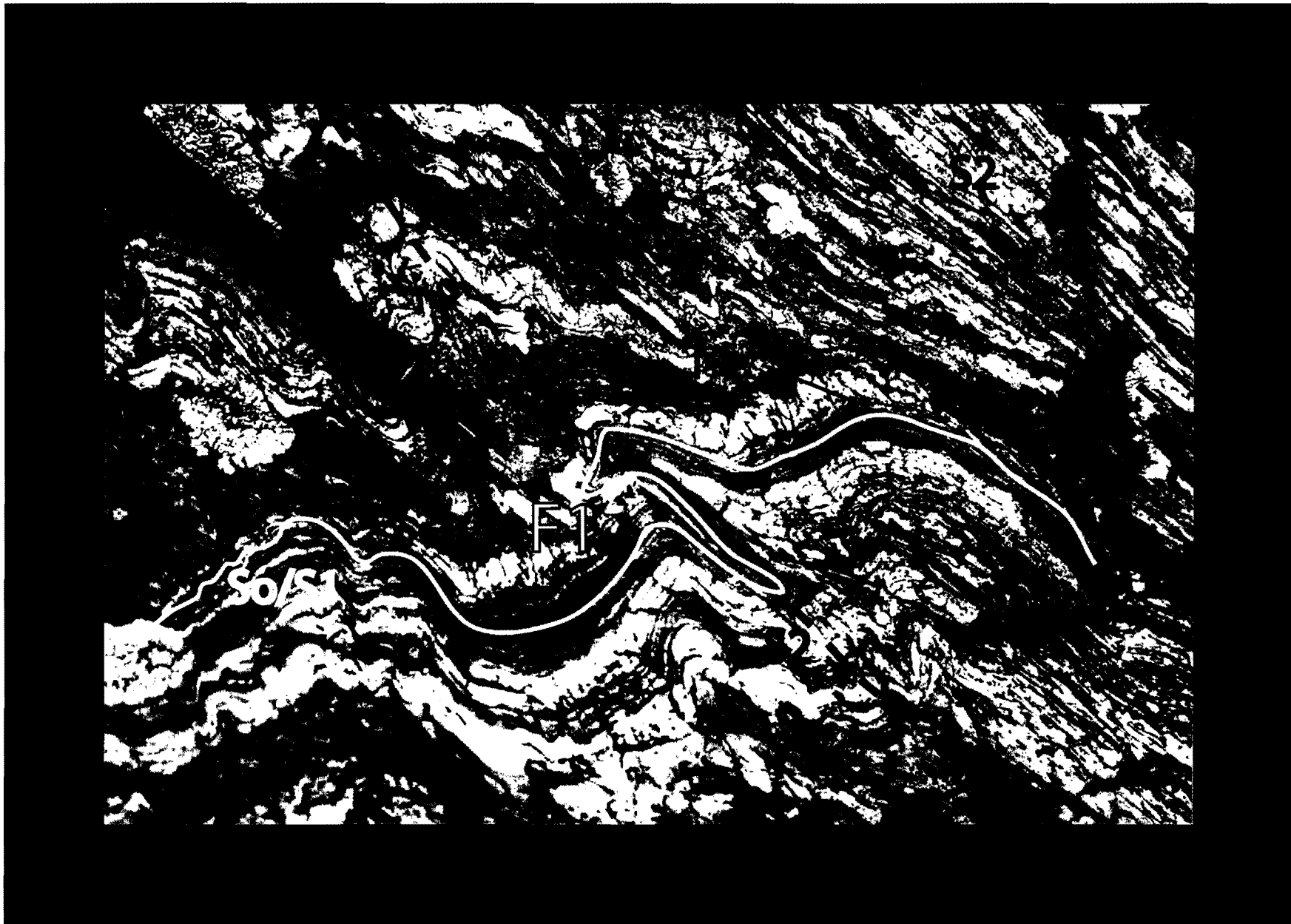


Figure 5: Photo of the nature of folding within the study area. So/S1 transposition layering has been folded by F1 folds and subsequently refolded by F2. The main penetrative fabric, S2, is NE striking, with NW-SE steep dip directions. The view of the photo is to the NE, parallel to S2. Rock type is banded metarhyolite. (Photo courtesy of K. Karlstrom)

My mapping within the Capilla Peak area was concentrated on tracing and linking-up quartzite marker beds and searching for primary structures (Cross bed sets and bedding) to determine younging direction. This work has introduced a new structural interpretation, which is illustrated by the accompanying appended cross-section. A major synclinorium is mapped beneath the MLSZ. Quartzite marker units are boudinaged and discontinuous, but preserved cross bedding in the quartzite units and bedding-cleavage relationships are used to interpret the folds. The photograph in figure 6 is an excellent example of preserved primary structures within quartzite. The development (and tightening) of the synclinorium has been interpreted to be due to movement along the MLSZ. New work suggests that top-NW movements took place during each deformational event (D1-D3). The earlier movements (D1) occurred after (perhaps soon after?) emplacement of the 1656 MA Monte Largo granite as shown by the presence of S1 in the granite.

Deformation within the Capilla Peak Quadrangle was apparently more complex and pervasive within the footwall of the Monte Largo shear zone, as the competent quartzite and banded metarhyolite layers here pinch out, fork, and are complexly thinned and boudinaged. The schematic map of figure 2 as well as appendix map shows distribution of quartzites and metarhyolites and displays the inconsistent nature of deformation above and below the MLSZ. Similar units in the hanging wall are more continuous, emphasizing the interpretation of inconsistent deformation across the MLSZ.



Figure 6: Photograph of preserved primary structures. Original bedding within the quartzites help to define overall structure of central Manzano synclinorium. Cross bedding provide younging directions for quartzite marker beds. In this picture, younging is up and the photo is taken looking down-dip of bedding surface, in the NW corner of Quad., where quartzite beds strike N-NE and dip E-SE, ~40-50 deg.

Microstructural Analyses

In order to evaluate movement sense along the MLSZ, an evaluation of microstructures is necessary. Samples taken were cut parallel to stretching lineation and perpendicular to foliation. Each thin section provides microstructural information on the nature and characteristics of deformation in the vicinity of the MLSZ.

Thin sections described in this section have been chosen as the best representations of rocks in the study area. Thin sections were made from hand samples taken directly from the MLSZ (KCP-00-18 & 19, in photomicrographs of fig.9 and in fig. 7a) and from in the vicinity of the MLSZ (K99-ML-5 and KCP-00-22 in figures 7 b, c) for comparison of microstructures within and outside of the shear zone. Microstructures were similar for samples in and around the MLSZ, except for more pervasive mylonitization for samples taken directly from the shear zone. Delta porphyroclasts of KCP-00-22 indicates shear sense and was consistent with top-to-the-northwest movement (see figure 7c). Grain size reduction can be seen in all samples.

Samples KCP-00-18 and 19 are mylonitized quartzites (Figures 7a & 9) that exhibit shear sense indicators as well as microstructures that can define the deformational regime of the MLSZ. The main fabric, S_2 , is defined by grain shape preferred orientations (GSPO) as well as by orientations of mica grains (photomicrographs of Figure 9). S-C fabrics within both of these samples indicate the top-to-the-northwest shear sense. Core and mantle features can be seen in sample KCP-00-18 (photomicrographs of Figure 9), which emphasizes grain boundary migration recrystallization during deformation. The existence of these microstructures suggests

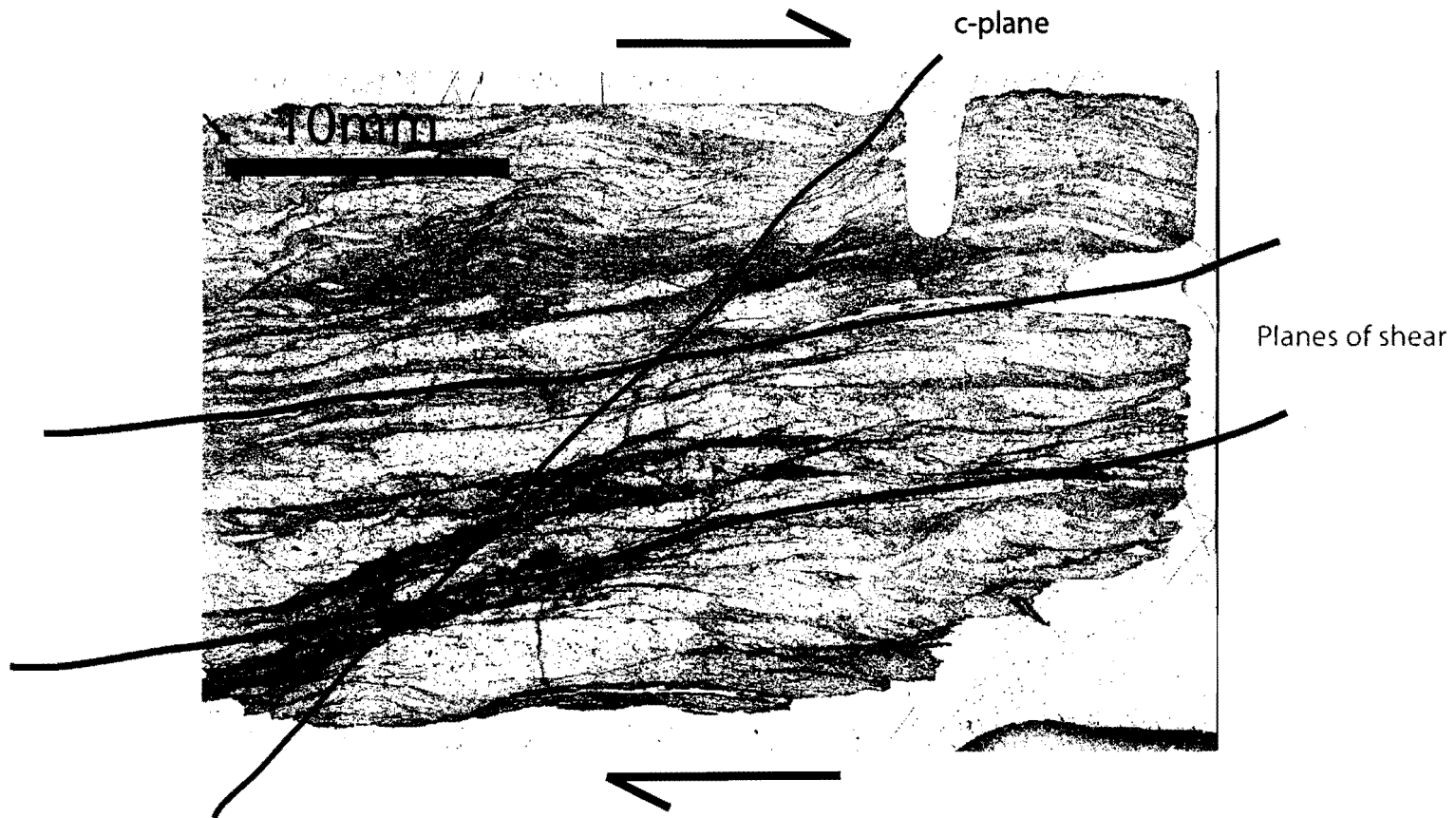
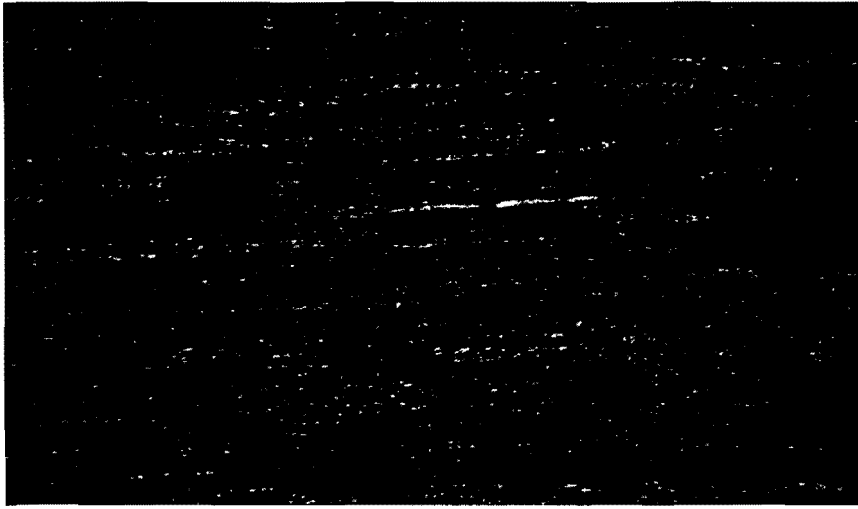


Figure 7a: Image of thin section from KCP-00-19, taken from the MLSZ. Thin section is cut perpendicular to foliation and to the planes of shear (parallel to stretching lineation). In general, view is looking SW along the MLSZ. Shear sense is top to the northwest indicated by s-c fabric.



~1mm

Figure7b: K99-ML-5 from near the MLSZ. Photomicrograph is 6x and view is looking down the planes of shear. Shear planes are well defined by quartz stringers. Grain size reduction is evident in this quartz mylonite.

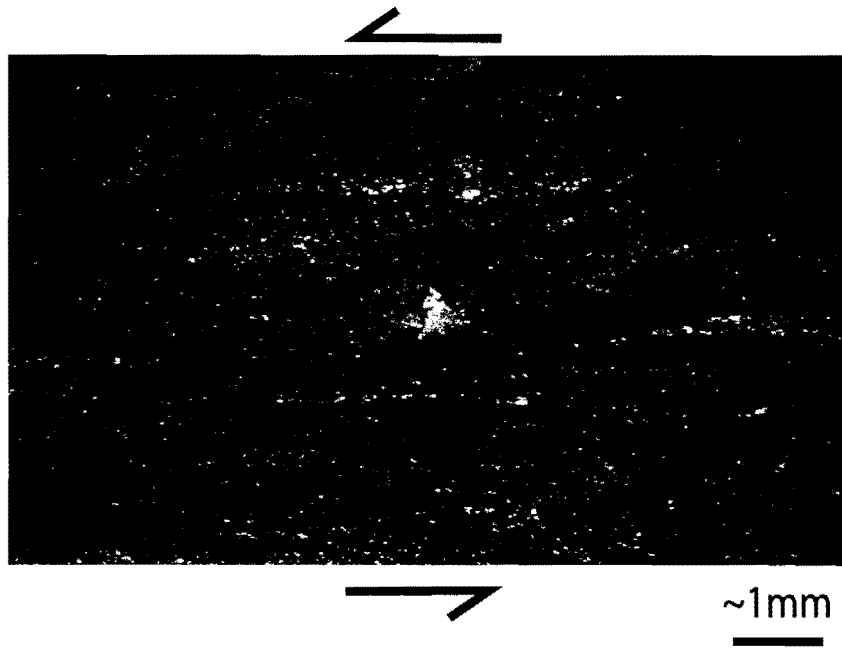


Figure 7c: KCP-00-22 taken from near the MLSZ. Photomicrograph is 6x and taken in X-polarized light. Delta porphyroblast in center of image has strain shadows indicating sense of shear.

moderate temperatures during deformation (350-450°C) and represent, generally, regime 2-3 deformation according to Hirth and Tullis, 1992.

All samples analyzed contain undulose extinction and grainsize reduction, exemplifying the intense deformed textural nature of these samples.

Geochronology

The technique of in situ monazite dating can be used in geochronological studies of deformed rocks. A component of many rocks, Monazite is a cerium phosphate mineral and is common among metamorphic rocks. One important aspect of monazite geochronology is the fact that mineral growth can be related to structural development. Relationships between individual grains and microstructural features are studied in situ, allowing the opportunity to gain an absolute date of individual deformational events. U-Th-Pb dates can be determined for individual monazite grains, and even particular portions of grains. The process of in situ monazite dating has several steps, including location of grains, determining compositional variation within each grain, and calculating radiometric dates based on the relative abundances of radiogenic elements (U-Th-Y-Pb). Once these elemental abundances are obtained, solving decay equation will obtain absolute ages (Montel et al., 1996)

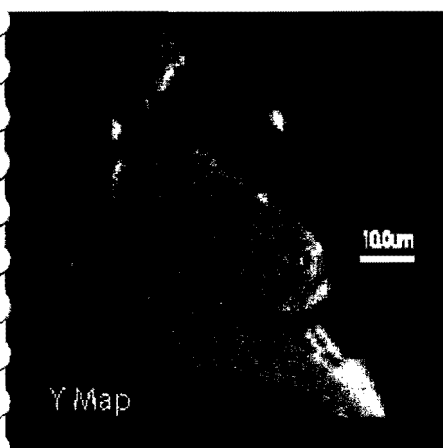
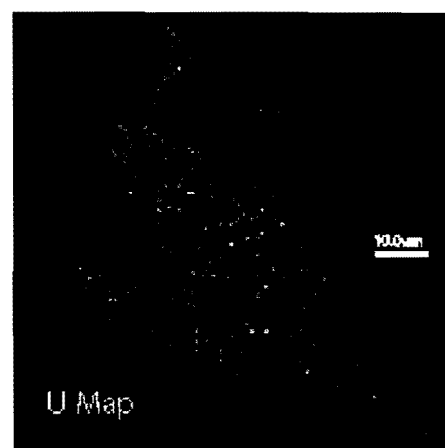
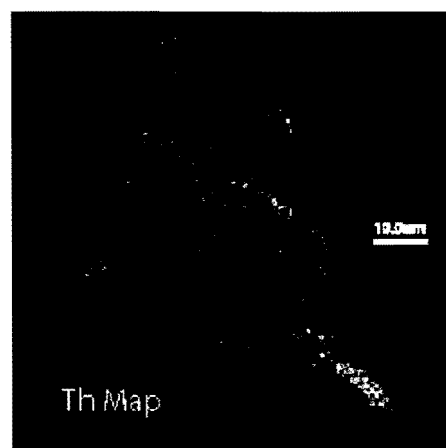
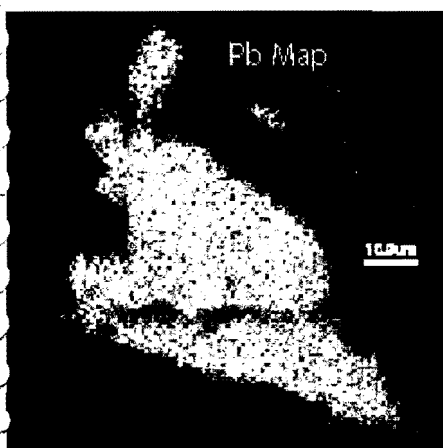
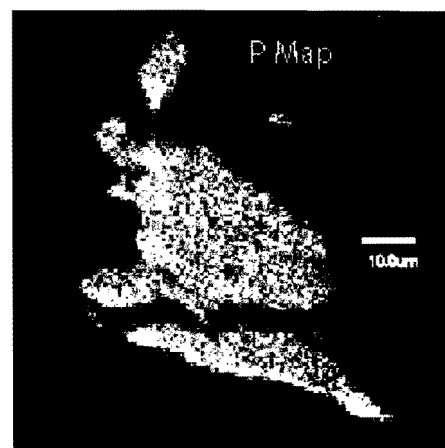
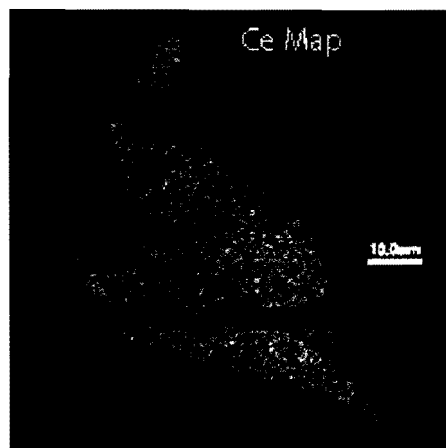
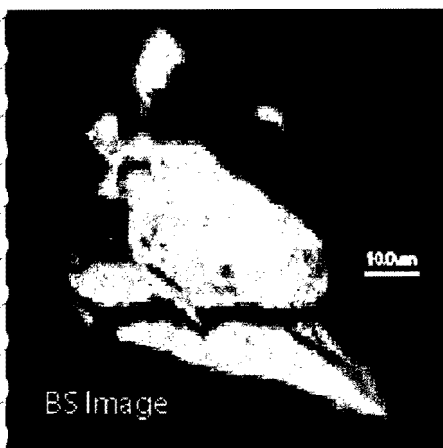
Within the process of determining absolute ages of individual monazite grains, several assumptions are taken before determining an age. The assumption that there is no common lead present within the crystal structure of the grain such that all Pb is the result of radiogenic decay processes occur insures that the concentration of Pb evaluated is generated only by decay of U, and Th (Parrish, 1990). Loss of Pb out of the grain is also

an important issue to address. Before determining ages, another assumption taken is that there is no lead loss out of the 'system' (Montel, 1996). The last assumption is that monazite is quite refractory, difficult to being 'reset,' and is essentially a closed system.

Thin sections cut and polished from an Xq sample taken from within the shear zone. Scanning Electron Microscopy at the facilities at UNM were used to locate monazite grains within the section. The microprobe at UNM was then used to make compositional maps of selected elements. Figures 8a, b, c are the compositional maps of each grain for various elements (Ce, P, Pb, Th, U, & Y). Although compositional zoning is quite common among monazites within polydeformed rocks, no discernible zoning was seen within these grains. The grain to be analyzed was chosen based, in part, on the significance of the position of the grain within the tectonic fabric. These particular grains were more precisely analyzed at the microscopy facilities at New to determine absolute ages of areas (<6um in dia.) within each grain. This technique of determining ages for domains within the grain is advantageous due to the ability to obtain statistical means of ages determined and evaluate possible polyphase history.

Sample KCP-00-19 was analyzed for the purposes of monazite geochronology. Three different monazite grains were chosen, based on the fact that they were the largest grains (1100-3000 μm), with the most regular surface, i.e. minimal cracks or pores, and exhibited the most regular perimeter surface. Features (grains from figs. 8 a, b, c) #sr547, 375, & 389 were scanned for U, Th, Y, Pb compositions and the resultant analyses are listed in appendix A.

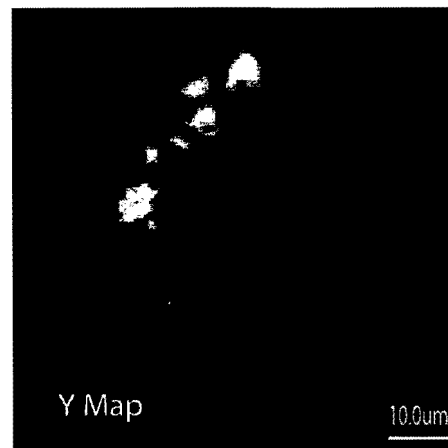
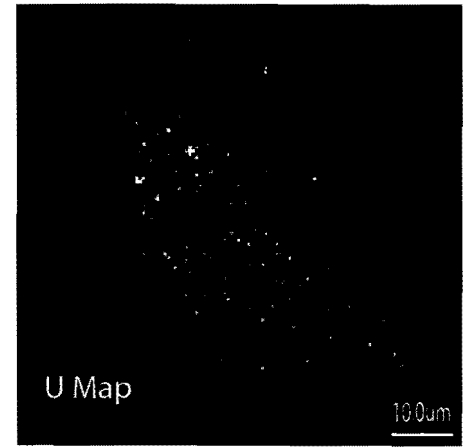
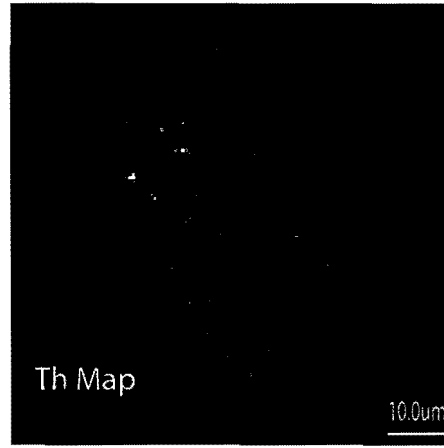
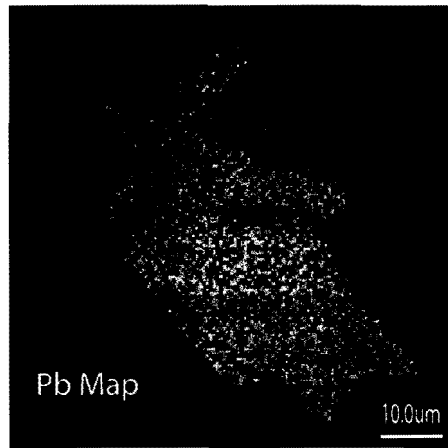
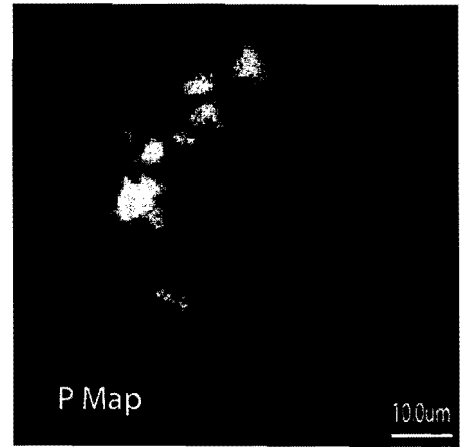
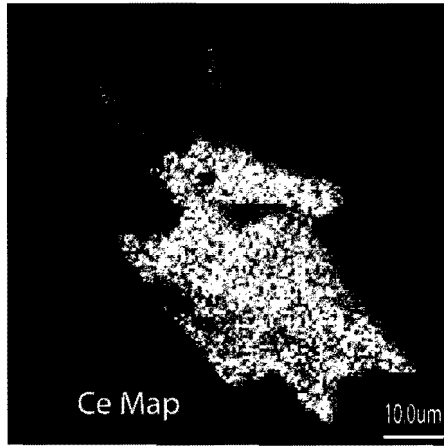
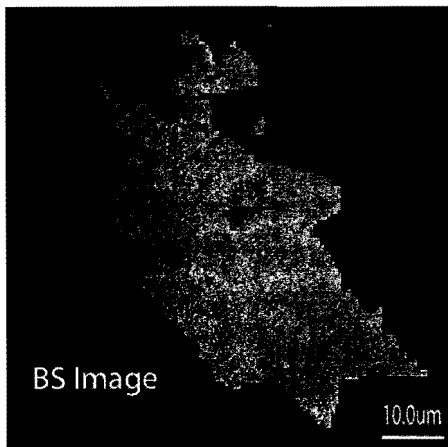
Ages were obtained for 7-9 spots on each grain, yielding 24 analyses. Spot analyses were distributed as equally as possible for the purpose of determining whether



Compositional Maps of Feature #375; Area: 1206um
Probe Coordinates: X=27.23 Y=33.27

Cracked and broken Mz grain

Figure 8a: Microprobe image of selected grain from grain #sr375, elements are relatively uniform throughout grain, showing no internal pattern of element distribution.

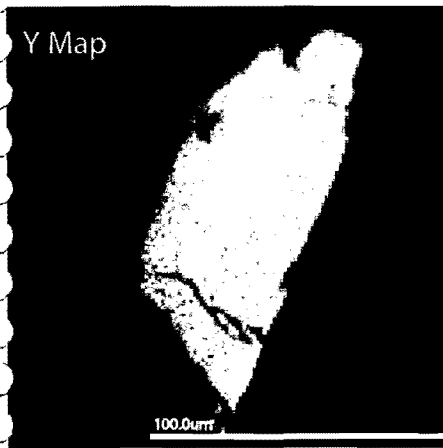
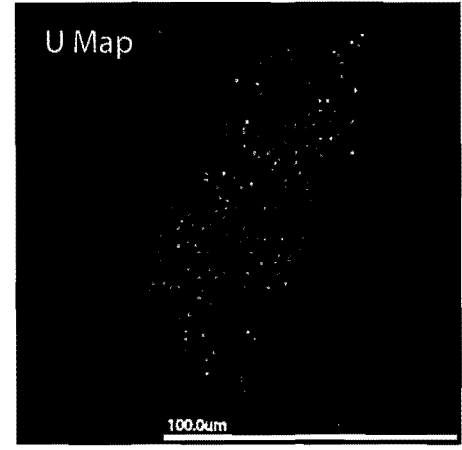
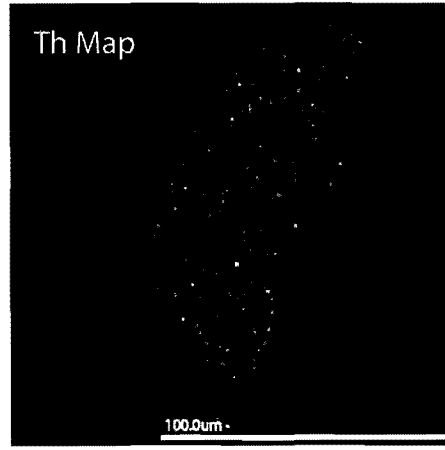
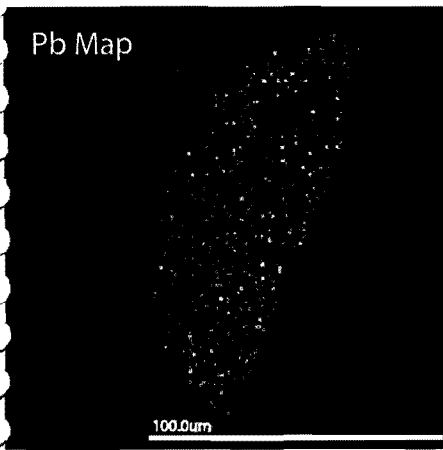
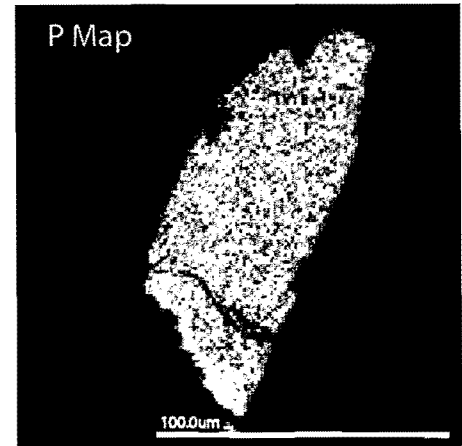
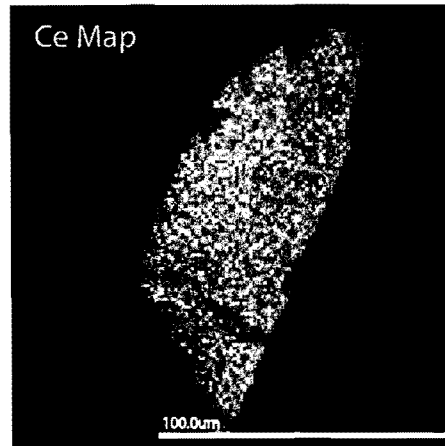
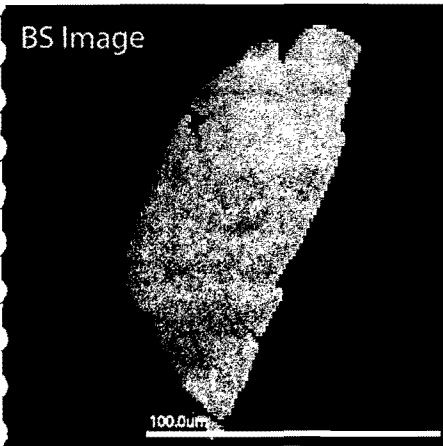


Compositional Maps of Feature #389; Area: 1191um

Probe Coordinates: X=15.83 Y=32.80

Grains of Xenotime and large Monazite

Figure 8b: Grain #sr389 is both Xenotime (speckled grains in upper-left corner of grain) and Monazite together. Consistent distribution of elements in Monazite with no discernible internal patterns.



Compositional Maps of Feature #547; Area: 3331um
Probe Coordinates: X=12.88 Y=22.96

Grain is aligned in main foliation, long axis parallel

Figure 8c: Regular distribution of elements in #sr547, with no internal pattern. This grain, however, is aligned within the S2 fabric.

or not each grain had recognizable age patterns, i.e. a younger core and older rims (if compositional zoning were actually present). The mean age determined was 1247 Ma. The results of the age determination for the three grains chosen are represented in Figures 9a, b, c. Another analysis conducted by M. Williams at the University of Mass., Amherst on a similar quartzite sample from the study area yielded a mean age of 1380 Ma, represented in Figure 10 (Williams, unpublished data). The majority of ductile movements on the shear zone took place at about ~1380 Ma, as shown by these new dates on syntectonic monazite grains (Williams et al., 2001). These dates are interpreted to be a time of shearing in the MLSZ.

Discussion

New mapping within the Capilla Peak Quadrangle has yielded the structural interpretation of a 'synclinorium' within Proterozoic rocks in the Manzano Mountains. Prominent quartzite marker beds preserving relevant primary structures have constrained the geometry of Proterozoic structures. Subsequent tightening of this synclinal feature took place during progressive long-lived movements along the Monte Largo shear zone.

The MLSZ is a major Precambrian structure within the central portion of the Manzanos, and is a thrust sense zone of ductile deformation. Beneath the zone of thrust, nappe-like F_1 folds are refolded by F_2 producing complex interference geometries as well as complex patterns in map view. Mesoproterozoic movement is accompanied by major fluid pulses reflected in the series of quartz veins within rocks surrounding the MLSZ. Coincident with the Mazatzal Orogeny (<1.65 Ga), pulses of movements have occurred along the MLSZ. The results of this preliminary geochronologic study of the kinematics

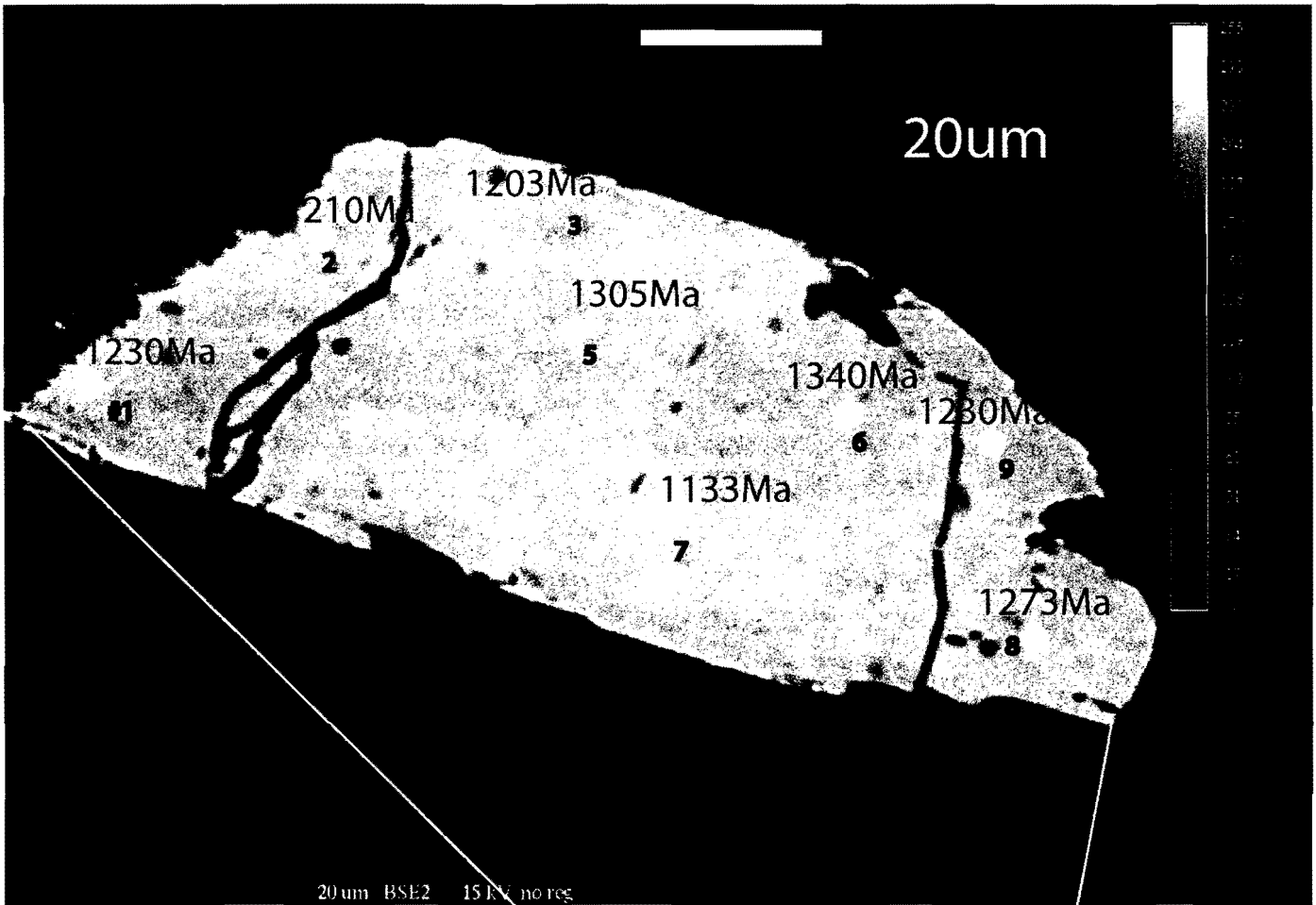
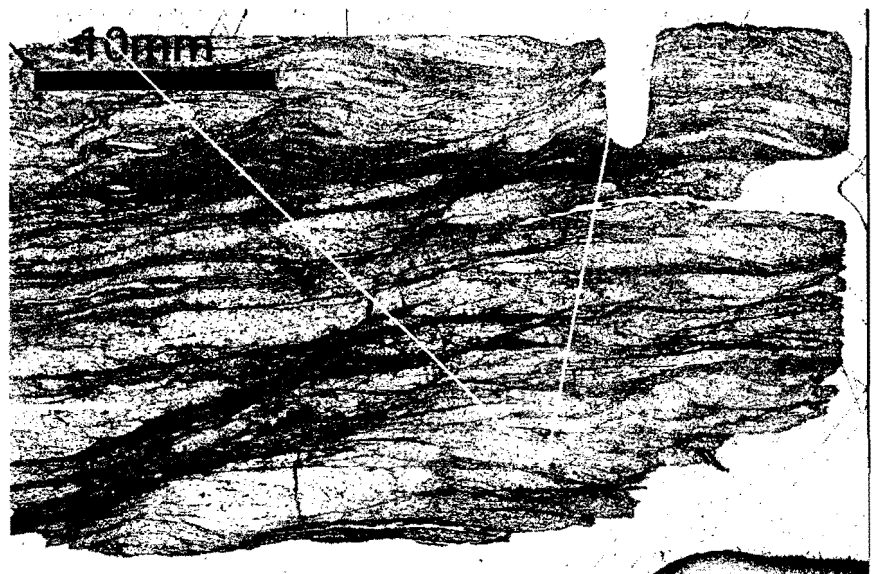


Figure 9a: Grain #sr547 is aligned within the fabric of S2, which is the main foliation of study and of the thin section (to right). The ages determined within this feature show no discernible pattern within the distribution of ages throughout the grain.



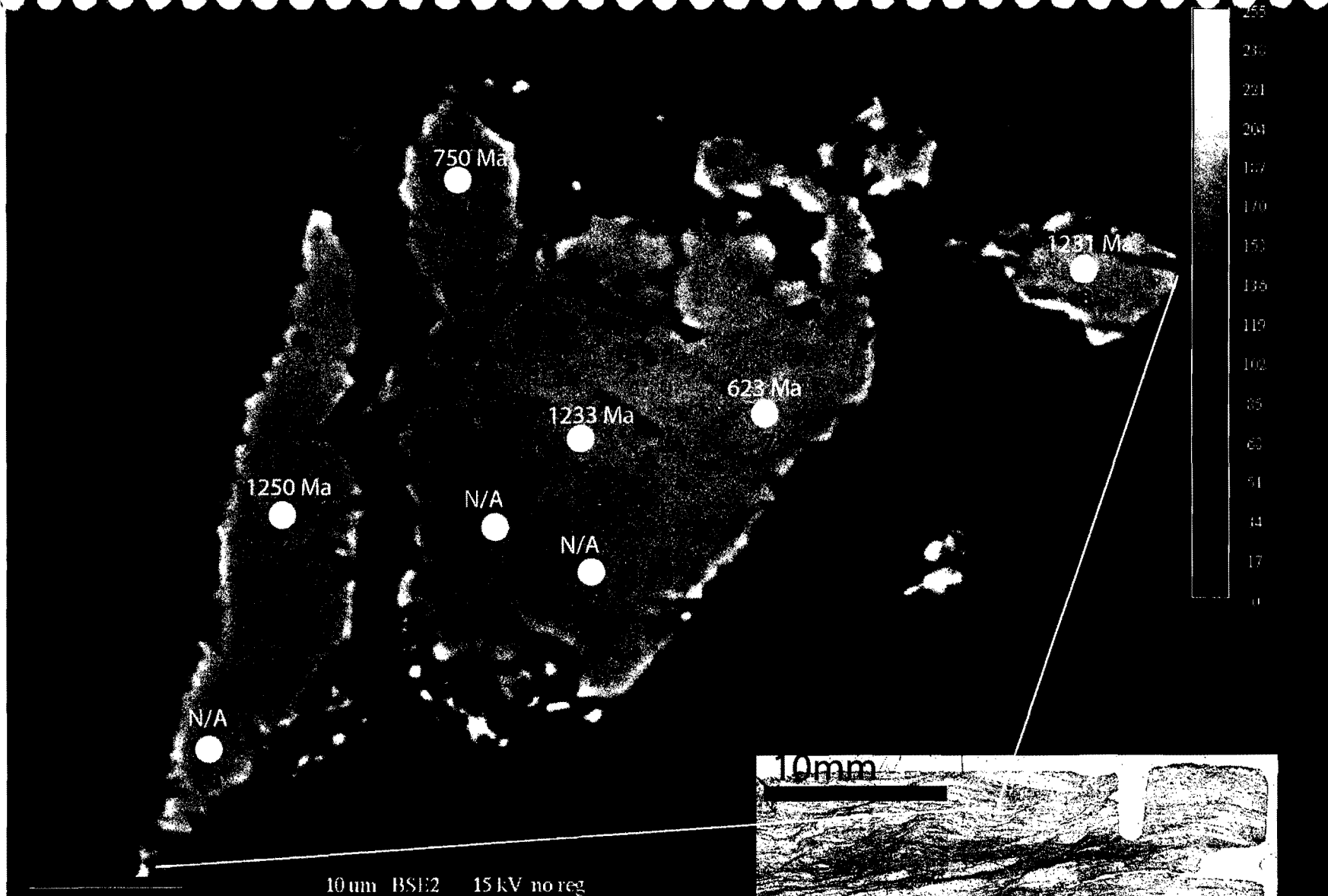


Figure 9b: Deformed grain #sr375 has no discernible age pattern. Furthermore, absolute age analyses sr375-3, 4, & 5 were unattainable.



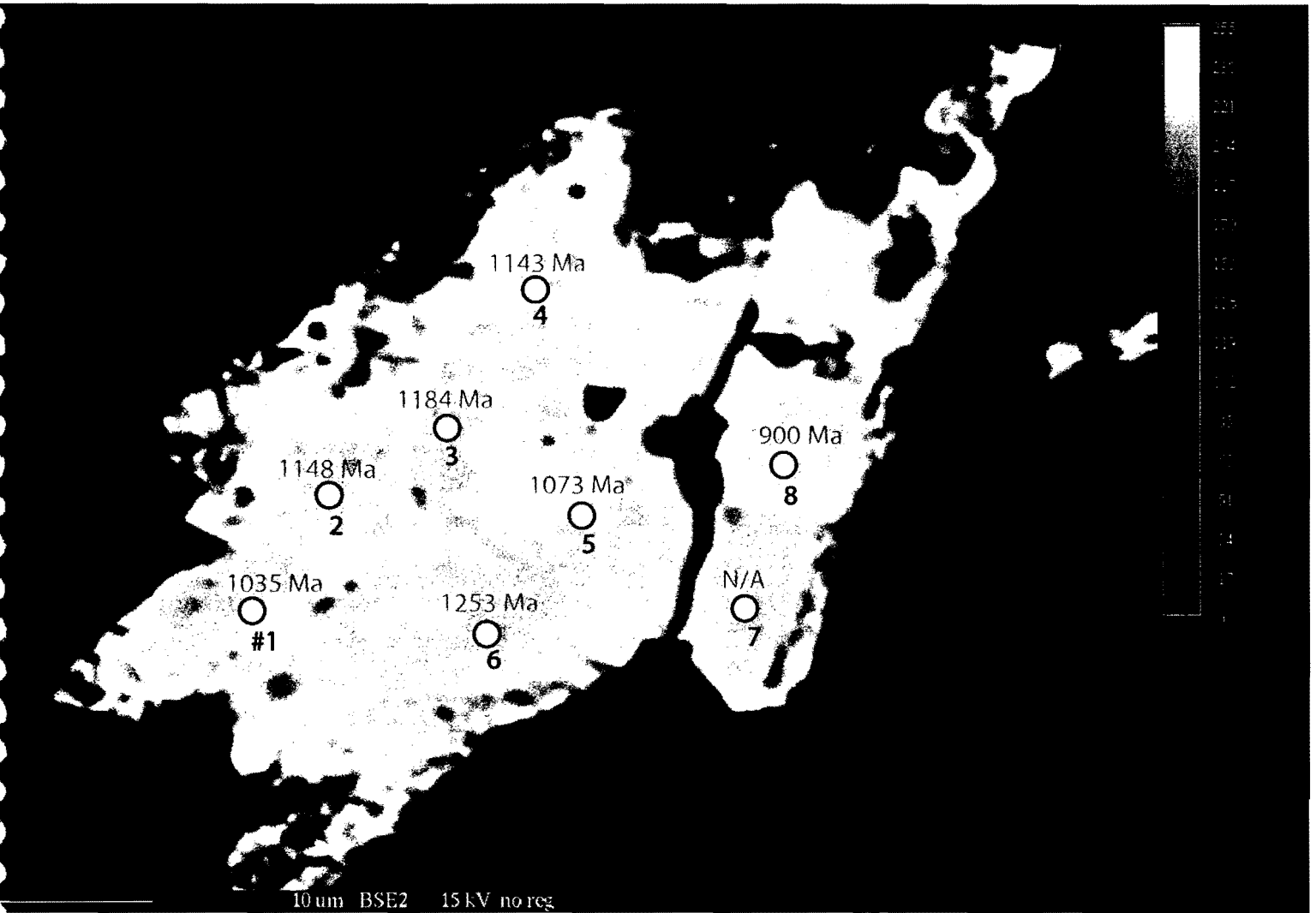


Figure 9c: #sr389 displays no discernible age pattern within its interior. Analysis for sr389-7 was unattainable.



KCP 0018 Monazite 1

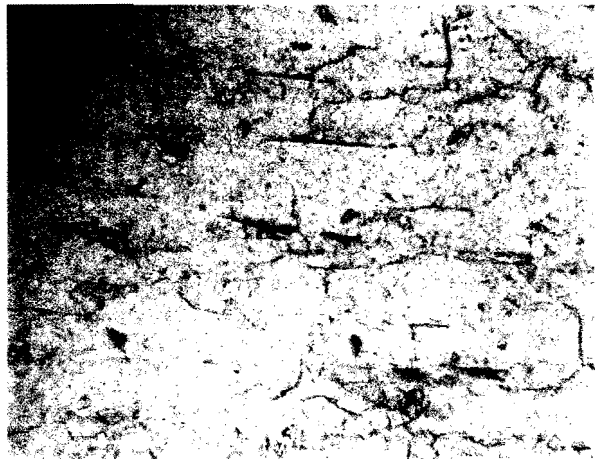
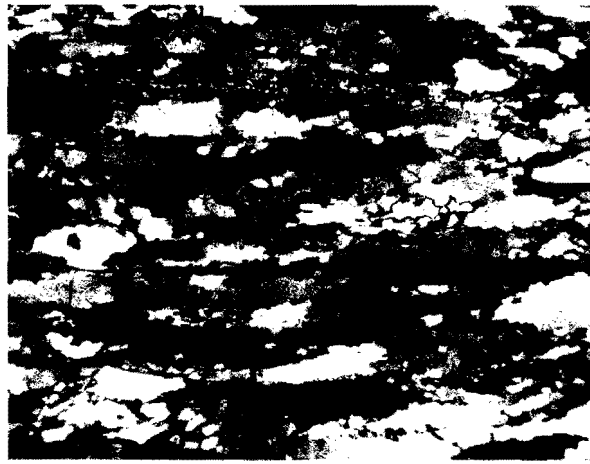
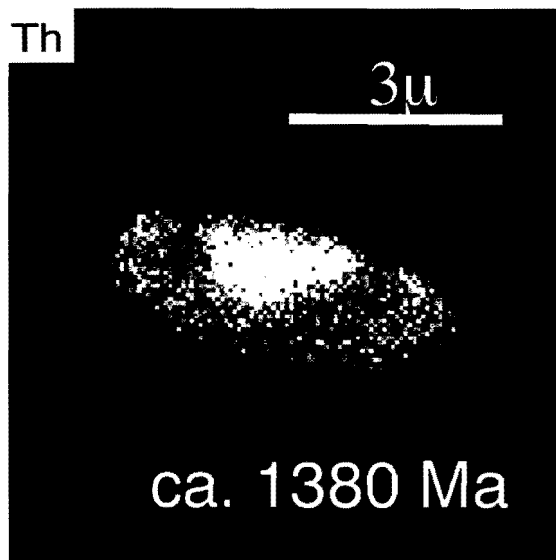
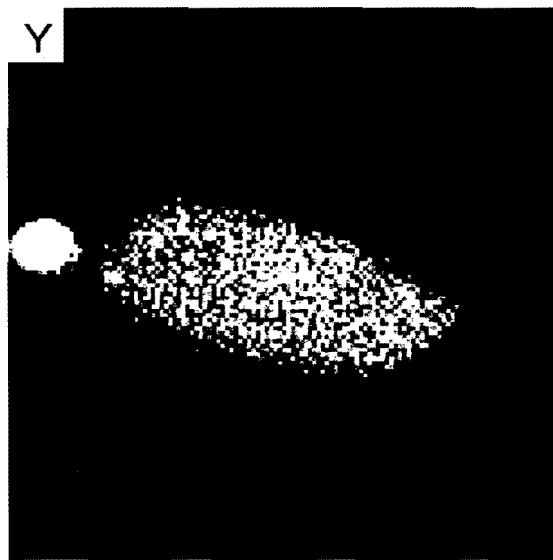


Figure 10: SEM images and photomicrographs of Monazite grains (top two) and microstructures in X-polarized light and plain light (lower right). Monazite grain has rim and core feature with mean age of ca. 1380 Ma. Undulose Quartz stringers with mantle/core microstructures are observed. Images courtesy of Williams, unpublished data.

of MLSZ, however, suggests that the majority of thrusting occurred >1.4 Ga. Fabrics contained within regional plutons, i.e. Ojito and Monte Largo (~ 1600 Ma) suggest the majority of regional deformation after emplacement of these plutons.

References

- Bauer, P. W., 1982, Precambrian geology and tectonics of the southern Manzano Mountains, Central New Mexico: New Mexico Geological Society, Guidebook to the 33rd Field Conference, p. 211-216.
- Bauer, P. W., Karlstrom, K. E., Bowring, S. A., Smith, A. G., Goodwin, L. B., 1993, Proterozoic plutonism and regional deformation- new constraints from the southern Manzano Mountains, Central New Mexico: New Mexico Geology v. 15, no. 3, p.49-56.
- Bauer, P. W., Pollock, T. R., 1993, Compilation of Precambrian isotopic ages in New Mexico: New Mexico Bureau of Mines and Mineral Resources, Open-file report 389, 130pp.
- Bowring, S. A., Karlstrom, K. E., 1990, Growth, stabilization, and reactivation of Proterozoic lithosphere in the southwestern United States: *Geology*, v.18, p.1203-1206.
- Hirth and Tullis, 1992. Dislocation creep regimes in quartz: *Journal of Structural Geology*, v. 14, p. 145-159.
- Karlstrom, K. E., Bowring, S. A., 1988, Early Proterozoic assembly of tectonostratigraphic terranes in southwestern North America: *Journal of Geology*, v.96, p.561-575.
- Karlstrom, K., Connell, S.D. and others, expected 2001, Geology of the **Capilla Peak** 7.5-min. quadrangle, Valencia and Torrance Counties, New Mexico, New Mexico Bureau of Mines and Mineral Resources, Open-file Geologic Map OF-GM 27, scale 1:12,000.
- Johnson, S. E., 1986, Structural Analysis and reinterpretation of an apparent Precambrian angular unconformity, central Manzano Mountains, New Mexico: *New Mexico Geology*, v.8, no.3, p.45-50.
- Montel, J. M., Foret, S., Veschambre, M., Nicollet, C., Provost, A., 1996, Electron microprobe dating of Monazite: *Chemical Geology*, v.131, p.37-53.
- Northrup, Clyde J., 1991, Thermal, chemical and structural characteristic of fluid migration and fluid-rock interaction in a mid-Proterozoic shear zone, Manzano mountains, New Mexico [Master's Thesis]. Dept. of Geosciences, Northern Arizona University, 125p.

- Parrish, R. R., 1990, U-Pb dating of monazite and its application to geological problems: Canadian Journal of Earth Sciences, v. 27, p.1431-1450.
- Raszewski, D. A., 1999, Polyphase tectonics and metamorphism and their relation to movement on the Monte Largo shear zone in the Manzano Mountains, central New Mexico [Senior Thesis]. Albuquerque, University of New Mexico, 33p.
- Thompson, A. G., Grambling, J. A., Dallmeyer, R. D., 1991, Proterozoic tectonic history of the Manzano Mountains, central New Mexico: New Mexico Bureau of Mines and Mineral Resources Bulletin, v. 137, p. 71-77.
- Thompson, A. G., Grambling, J. A., Karlstrom, K. E., Dallmeyer, R. D., 1996, Mesoproterozoic metamorphism and $^{40}\text{Ar}/^{39}\text{Ar}$ thermal history of the 1.4 Ga Priest pluton, Manzano Mountains, New Mexico: The Journal of Geology, v.104, p.583-598.
- Williams, M. L., Karlstrom, K. E. Jercinovic, M. J., Stevens, L., 2001. Microprobe Monazite geochronology from the Manzano Mountains, New Mexico: Distinguishing stages in a long-live and reactivated orogen. GSA Abstracts w/Pograms, Rocky Mountain and South-Central Sections, v. 33, n. 5.

Y,Th,U,Pb point analyses from monazite grains Name: Steven Rogers

Date: 4/20/01

Decay Constants

Th232 5E-11

U238 2E-10

U235 1E-09

Analytical parameters:

acquisition time:

bias (sp3):





other:

| ID number | Anal # | Analysis (ppm) | | | | Calc | | Individual Age Terms (n=3) | | 238 Age (4-digit Mean Value (x'tal Std.Dev. (x'tc 1sigma (+/-) | |
|-----------|--------|----------------|-------|-----|------|---------|-----------|----------------------------|-------------|--|-----------|
| | | Y | Th | U | Pb | Pb cor | Pb | 232 | 238 | | |
| sr547-1 | #17 | 4100 | 8230 | 100 | 490 | 482.62 | 482.75971 | 463.205368 | 18.05843727 | 1247.111111 | 59.978597 |
| sr547-2 | #18 | 3400 | 4980 | 40 | 290 | 283.88 | 283.26805 | 275.591749 | 7.094562093 | | |
| sr547-3 | #19 | 2990 | 8240 | 60 | 470 | 464.618 | 464.72023 | 453.281867 | 10.57435789 | | |
| sr547-4 | #20 | 3010 | 5280 | 0 | 320 | 314.582 | 314.63438 | 314.634382 | 0 | | |
| sr547-5 | #21 | 5000 | 2140 | 400 | 220 | 211 | 211.76565 | 128.028751 | 77.09997398 | | |
| sr547-6 | #22 | 5070 | 2670 | 260 | 230 | 220.874 | 220.2915 | 164.164632 | 51.60371036 | | |
| sr547-7 | #23 | 5100 | 7900 | 350 | 480 | 470.82 | 470.90285 | 408.575991 | 57.77053257 | | |
| sr547-8 | #24 | 4350 | 8540 | 170 | 540 | 532.17 | 532.5733 | 497.991444 | 31.88213681 | | |
| sr547-9 | #25 | 3530 | 5330 | 70 | 270 | 263.646 | 313.67402 | 299.985979 | 12.64090609 | | |
| sr375-1 | #26 | 3150 | 2710 | 20 | 100 | 94.33 | 94.154656 | 91.8962173 | 2.119759499 | | |
| sr375-2 | #27 | 4710 | 3310 | 60 | 210 | 201.522 | 201.37098 | 189.419122 | 11.02888189 | | |
| sr375-3 | #28 | 2370 | 720 | 0 | 0 | -4.266 | 0 | 0 | 0 | | |
| sr375-4 | #29 | 2980 | 550 | 30 | 0 | -5.364 | 0 | 0 | 0 | | |
| sr375-5 | #30 | 4070 | 980 | 170 | 10 | 2.674 | 0 | 0 | 0 | | |
| sr375-6 | #31 | 3900 | 9430 | 310 | 600 | 592.98 | 592.86686 | 532.07883 | 56.13116772 | | |
| sr375-7 | #32 | 2940 | 4060 | 10 | 120 | 114.708 | 114.92627 | 114.000914 | 0.871626019 | | |
| sr375-8 | #33 | 3360 | 18010 | 300 | 1080 | 1073.95 | 1073.2159 | 1014.49815 | 54.22369534 | | |
| sr389-1 | #34 | 3710 | 4260 | 20 | 210 | 203.322 | 203.98883 | 200.771928 | 2.992166278 | | |
| sr389-2 | #35 | 6310 | 10400 | 130 | 580 | 568.642 | 568.69502 | 545.197453 | 21.76775981 | | |
| sr389-3 | #36 | 7140 | 21210 | 210 | 1200 | 1187.15 | 1187.1016 | 1147.78789 | 36.37043387 | | |
| sr389-4 | #37 | 5510 | 5620 | 40 | 310 | 300.082 | 300.49083 | 293.296503 | 6.665939022 | | |
| sr389-5 | #38 | 4900 | 7630 | 230 | 420 | 411.18 | 411.67508 | 373.155035 | 35.78142344 | | |
| sr389-6 | #39 | 3400 | 19310 | 180 | 1150 | 1143.88 | 1143.73 | 1107.77545 | 33.17402012 | | |
| sr389-7 | #40 | 3870 | 1720 | 80 | 30 | 23.034 | 0 | 0 | 0 | | |
| sr389-8 | #41 | 2640 | 10560 | 30 | 440 | 435.248 | 435.44983 | 431.317223 | 3.861168325 | | |

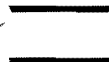









Appendix A: Data table of calculated ages of domains in Monazite grains from sample KCP-00-19.

Explanation

Lithologic Units

-  Quaternary Alluvium
- Paleozoic Rocks**
-  Pmu Madera Group, upper arkosic unit
-  Pml Madera Group, lower cherty limestone unit
-  Ps Sandia Formation

Proterozoic Rocks

-  Xml Monte Largo granite
-  Xog Ojito Granite
-  Xbs Blue Springs Formation schist
-  Xr Metarhyolite (banded)
-  Xq Sais quartzite
-  Xwr White Ridge quartzite
-  Xla Lithic Arenite
-  Xps Pelitic Schist
-  Xa Sevilleta metavolcanic
Amphibolitic unit
-  Xsr Sevilleta metavolcanic
Metarhyolite unit (massive)

Map Symbols

